$[4Fe\text{-}4X]^{2+}$ (X = Sulfur, Selenium) Clusters in *Clostridium pasteurianum* Ferredoxin and in Synthetic Analogues: Structural Data from Resonance Raman Spectroscopy†

Jean-Marc Moulis,* Jacques Meyer, and Marc Lutz

ABSTRACT: Low-temperature (ca. 20 K) resonance Raman (RR) spectra have been recorded for $[4Fe\text{-}4X]^{2+}$ (X = S or Se) clusters of *Clostridium pasteurianum* ferredoxin and of synthetic analogues. Spectra of the native and of the Se-substituted ferredoxin display 10 and 11 bands, respectively, in the Fe–X stretching range. Assignments for the fundamental modes of these ferredoxins are proposed, based on the following grounds. Isotopic substitutions on core chalcogenide atoms ($^{32}S^* \rightarrow {}^{34}S^*$ and $^{76}Se^* \rightarrow {}^{82}Se^*$) permit the assignment of eight bands to Fe–X* stretching modes for each ferredoxin and the others to Fe–Scys stretching modes. The latter occur at frequencies ca. 10 cm^{-1} higher for the Se-substituted than for native ferredoxin. Polarization measurements, using ammonium sulfate as an internal standard, have been carried out on frozen solutions of both ferredoxins. Additional evidence for the assignments of totally symmetric modes is given by the spectra of $[Fe_4X_4(SC_6H_5)_4]^{2-}$ compounds in frozen acetonitrile solution, which display resonance essentially via A-term scattering when excited near their absorption maximum. RR spectra of $[Fe_4X_4(SCH_2CH_2CONH_2)_4]^{2-}$ derivatives in frozen aqueous solution were also studied. The present Raman data are consistent with the existence, in all $[4Fe\text{-}4X]^{2+}$ clusters investigated here, of a mainly tetragonal distortion lowering the symmetry from the idealized T_d to the D_{2d} point group. In particular, the S* → Se* substitution does not modify the symmetry of the cubane clusters in frozen solution, neither in synthetic analogues nor in proteins.

Iron–sulfur centers of the [4Fe-4S] type are distributed over an exceptionally wide range of organisms and enzymes. The properties of $[Fe_4S_4]$ clusters in proteins (Sweeney & Rabinowitz, 1980) and in synthetic analogues (Berg & Holm, 1982) have been extensively studied by a variety of physical and chemical methods. A wealth of structural information has been brought forth by X-ray crystallographic investigations of several proteins (Adman et al., 1976; Carter, 1977a; Stout, 1982). However, our understanding of the exact conformation of the clusters in proteins remains limited to the data obtained on crystals and additional information is highly desirable. Resonance Raman (RR)[1] spectroscopy, which is a very selective and sensitive structural probe of chromophores in biological systems (Spiro & Gaber, 1977), whatever their physical state, can potentially provide such information (Spiro et al, 1982). The quality of early RR spectra of [4Fe-4S] clusters (Tang et al., 1975) was limited by experimental difficulties, but significant progress has been achieved recently, allowing band assignments based on $^{32}S \rightarrow {}^{34}S$ isotopic substitutions (Johnson et al., 1982b; Spiro et al., 1982). Further improvements have been made by working at low temperature, and heretofore undetected bands have been observed, particularly in spectra of the 2[4Fe-4S] Fd from *Clostridium pasteurianum* (Lutz et al., 1983; Johnson et al., 1983; Moulis et al., 1984).

We report here measurements of $^{32}S^* \rightarrow {}^{34}S^*$ isotopic shifts and depolarization ratios, carried out on these low-temperature spectra. Similar experiments, with ^{76}Se and ^{82}Se isotopes, have been extended to the 2[4Fe-4Se] Fd from *C. pasteurianum*, which has recently been prepared and characterized (Meyer & Moulis, 1981; Moulis & Meyer, 1982). The substitution of the bridging sulfur atoms of the cubane-like core by selenium does not significantly modify the biological properties of the active site (Moulis & Meyer, 1982) but is expected to largely alter its vibrational behavior in part because of the larger atomic weight of selenium compared to sulfur. For the sake of comparison, we have recorded RR spectra of synthetic $[Fe_4X_4]^{2+}$ clusters dissolved in water or in acetonitrile. These data have been used for the assignment of 10 Fe–X or Fe–Scys stretching bands of the [4Fe-4X] clusters in the 150–400-cm^{-1} frequency range.

Materials and Methods

The ferredoxin from *C. pasteurianum* W5 (ATCC 6013) was purified and apo- and Se-substituted proteins were prepared according to published procedures (Moulis & Meyer, 1982). Elemental ^{34}S (95 %), ^{76}Se (99.5 %), ^{77}Se (92%), and ^{82}Se (92 %) were purchased from the Commissariat à l'Energie Atomique, Saclay, France, and Cp Fd samples enriched in these isotopes were obtained by a modification of a published method (Fee et al., 1971): the chalcogenide solution was prepared by heating the free element in a closed vessel under a hydrogen atmosphere until all the solid had reacted. After the vessel had cooled, a stoichiometric amount of DTT in aqueous solution was injected to solubilize the products. The apoferredoxin and ferric chloride solutions were subsequently added to the same vessel to initiate the reconstitution reaction, which was carried on as previously described (Moulis & Meyer, 1982). Fd samples of ca. 1 mg in 50 mM potassium phosphate buffer, pH 7.5, were concentrated to ca. 100 μL on a Diaflo YM2 (Amicon) ultrafiltration membrane, lyophilized, and kept under argon in sealed ampules.

3-Mercaptopropionamide was prepared as described previously (Miller et al., 1971). $[(C_2H_5)_4N]_2[Fe_4X_4(SR)_4]$ compounds (R = $-C_6H_5$, $-CH_2CH_2CONH_2$) were synthesized

† From the DRF/Biochimie (INSERM U.191), Centre d'Etudes Nucléaires de Grenoble, 38041 Grenoble Cedex, France (J.-M.M. and J.M.), and DB/Biophysique, Centre d'Etudes Nucléaires de Saclay, 91191 Gif-sur-Yvette Cedex, France (M.L.). *Received April 5, 1984.* This research was supported in part by funds from the CNRS (A.P. PIRSEM 1105, 1107, and 3075).

[1] Abbreviations: RR, resonance Raman; X, sulfur or selenium; X*, S*, and Se*, bridging chalcogenide atoms of the inorganic core; Scys, cysteine sulfur; S_t, sulfur atoms of the thiolate ligands; Cp, *Clostridium pasteurianum*; Fd, ferredoxin; DTT, dithiothreitol; HSpa, 3-mercaptopropionamide; Ph, phenyl; ρ_{app}, apparent depolarization ratio; ρ_{int}, intrinsic depolarization ratio; HiPIP, high-potential iron protein; ν(A–B), stretching mode of the A–B bond.

0006-2960/84/0423-6605$01.50/0

by using elemental sulfur or selenium (Christou et al., 1978; Christou & Garner, 1979) and recrystallized from acetonitrile.

Just before the RR experiments, the dry samples were dissolved in 10–20 μL of degassed solvent, quickly frozen on a microscope cover slip held over boiling liquid nitrogen, and introduced into a cryostat flushed with cold helium gas. The solvent was distilled water for the proteins, a 0.5 M aqueous solution of 3-mercaptopropionamide (pH 8.6) for $[Fe_4X_4(Spa)_4]^{2-}$ clusters, and acetonitrile for $[Fe_4X_4(SPh)_4]^{2-}$ clusters. The concentrations of [4Fe-4X] clusters were in the 5–50 mM range for all investigated samples. Temperatures were measured with accuracies close to 2 K by a calibrated resistor placed in the vicinity of the sample and were kept constant by adjusting the flow of helium.

Resonance Raman spectra were obtained by using grazing excitation on optically dense samples (Lutz, 1977). No cell wall was interposed on the path of the excitation beam in the sample area, thus avoiding any troublesome contribution from the Raman scattering of glass in the 300–500 cm^{-1} region (Lutz et al., 1983). The 457.9-nm emission from an argon laser (Spectra Physics 170.05) was filtered through a three-prism monochromator (Anaspec) and a narrow-band interference filter. The radiant power reaching the sample was about 1 mW, and light scattered was analyzed at about 90° from the illumination beam. The Raman spectrometer (Jobin-Yvon HG 2S-UV) was equipped with a d.c. detection. Typical spectral resolution was 6 cm^{-1} at 300 cm^{-1}. The frequencies were calibrated with the Rayleigh scattering (0 cm^{-1}) and the plasma lines of the Ar laser after removal of the interference filter. Spectra recorded with different samples of a given protein, including some containing ammonium sulfate (2.5 M), the strong 983-cm^{-1} band of which can be used as an internal standard (see below), showed that the frequencies of the RR bands were reproducible within less than 1 cm^{-1}. The signal to noise ratios were improved by summation of spectra in a multichannel analyzer (Tracor-Northern 1710).

Frozen aqueous solutions constitute strongly scattering and hence depolarizing media. However, the Raman lines observed often remained noncompletely depolarized, and the values of the apparent depolarization ratios (ρ_{app}) could be used to determine the intrinsic depolarization ratios (ρ_{int}), provided that internal depolarization standards could be measured. A simple relation may be used for this determination by assuming that the following hypotheses are satisfied: (i) the scattering, depolarizing medium can be considered as nonmacrocrystalline, i.e., it introduces no dephasing between differently oriented, plane-polarized waves and it depolarizes them to the same extent; (ii) the extent of depolarization of plane-polarized waves does not depend on their intensities. In these conditions, an incident plane-polarized light wave of intensity $I_\parallel$ emerges from the depolarizing medium as a wave having a component parallel to the incident polarization of intensity $I_\parallel - kI_\parallel$ and a perpendicular component of intensity $k'I_\parallel$, with $0 \leq k' \leq k \leq 1$. An incident plane-polarized wave of intensity $I_\perp$ perpendicular to the preceding one emerges as a wave with a $\perp$ component of intensity $I_\perp - kI_\perp$ and a $\parallel$ component of intensity $k'I_\perp$. The apparent depolarization ratio of a Raman band measured in these conditions is

$$\rho_{app} = \frac{I_\perp - kI_\perp + k'I_\parallel}{I_\parallel - kI_\parallel + k'I_\perp}$$

The intrinsic depolarization ratio of the same band is $\rho_{int} = I_\perp/I_\parallel$, and, hence

$$\rho_{app} = \frac{\rho_{int} + K}{K\rho_{int} + 1} \quad (1)$$

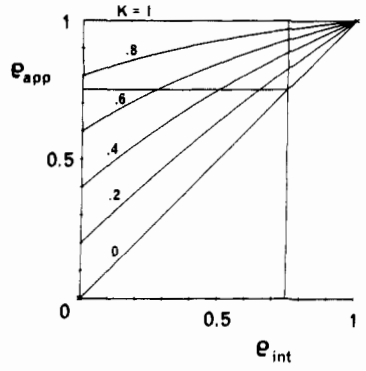

FIGURE 1: Dependence of ρ_{app} on ρ_{int} as a function of K. The curves have been drawn following eq 1 for six values of K (see the text).

with $K = k'/(1 - k)$. Relation 1 has been plotted in Figure 1 for six values of K in the 0–1 range and for $0 \leq \rho_{app}$ and $\rho_{int} \leq 1$. The depolarization ratios of the Fd bands were measured in the same experimental conditions as those used for obtaining nonpolarized spectra, except for ammonium sulfate (2.6 M for native Fd and 2 M for ^{77}Se-substituted Fd) being added as an internal depolarization standard. The scattered light was analyzed through sheet polarizers. Artifacts due to the differential sensitivity of the spectrometer to perpendicular ($\perp$) and parallel ($\parallel$) polarized lights were avoided by rotating the plane-polarized output from the $\perp$ polarizer by 90° by using an achromatic half-wave plate. The apparent depolarization ratios of the 983-cm^{-1} ($\rho_{int} \leq 0.05$) and 455-cm^{-1} ($\rho_{int} = 0.75$) bands of $(NH_4)_2SO_4$ in frozen solutions of the proteins provided evaluations of the K value and, hence, the correction factor for the measured ρ_{app} of the Fd bands (Figure 2; Tables I and II). For a given sample, the K values determined from each of the $(NH_4)_2SO_4$ bands were within 15% of each other, which suggests a good agreement with the proposed model. The accuracy of the ρ_{app} measurements largely depends on the intensities of the bands and on their mutual overlapping: in each case, extreme values were considered, thus affording an estimation of the uncertainty. The latter, when combined with the error on the K value, yielded the uncertainties of ρ_{int} that are given in Tables I and II.

Results

All of the RR spectra reported here were obtained with a laser excitation wavelength of 457.9 nm, which is on the low-energy side of the electronic absorption band centered at ca. 380 nm for $[4Fe\text{-}4X]^{2+}$ species in aqueous solution (Moulis & Meyer, 1982). This excitation wavelength was found to be efficient in promoting resonance of Raman-active modes of iron–chalcogenide clusters (Spiro et al., 1982; Lutz et al., 1983; Moulis et al., 1984).

$[4Fe\text{-}4S]^{2+}$ Centers of C. pasteurianum Fd. The low-temperature RR spectrum of oxidized Cp Fd excited at 457.9 nm (Figure 3A) displays a strong 340-cm^{-1} band and two sets of five and four weaker bands in the 250–300- and 350–400-cm^{-1} ranges, respectively: 10 lines are thus detected in the 250–400-cm^{-1} region (Table I). At lower frequencies, a weak and broad band is observed at 145 cm^{-1}. At higher frequencies, three very weak and ill-defined features are reproducibly observable at ca. 475, 535, and 570 cm^{-1}. In the 600–3000-cm^{-1} region (Figure 3A), the spectrum is blank, which confirms the resonance-enhanced origin of the [4Fe-4S] chromophore bands, without any Raman contribution from the polypeptide chain. The present low-temperature spectra of oxidized Cp Fd (Figure 3A) display more bands than those published previously (Spiro et al., 1982). This is due neither to any

Table I: Resonance Raman Frequencies (cm^{-1}) of [4Fe-4S]$^{2+}$ Clusters in Cp Fd and in Synthetic Analogues[a]

$Fe_4S_4(SPh)_4^{2-}$ [b]	$Fe_4S_4(Spa)_4^{2-}$ [c]	Cp Fd	isotopic shifts, $10^3 \times \Delta\nu/\nu$	depolarization ratios[d]	assignments, D_{2d}
145[e] vs[f]		145 w, br			
205 vw					
230 ew		232[g] w, br			
244 ew					
265 w sh	251 w	252 (4.5[h]) m	18 ± 4	0.77 ± 0.1	E
276 m		269 (4) w	15 ± 4	0.35 ± 0.2	A_1 } Fe-S*
	286 m	280 (4) w	14 ± 4	0.65 ± 0.2	B_1
293 w	295 sh	286 (4) vw sh	14 ± 4	0.6 ± 0.3	$B_2 + E$ }
		301 (6) vw	20 ± 4	n.d.	
	324 sh				
345 s	338 s	340 (6) s	18 ± 3	0.26 ± 0.1	A_1 Fe-S*
		353 (0) m	0	0.63 ± 0.2	$B_2 + E$ } Fe-Scys
368 ew	362 m sh	365 (1) m	3 ± 3	0.48 ± 0.2	A_1 }
	386 m sh	384 (6.5) w	17 ± 3	0.46 ± 0.2	$B_2 + E$ Fe-S*
	397 m	398 (5) w	13 ± 3	0.46 ± 0.2	
435 vs					
480 vw, br		475 w, br			
		535 w, br			
	567 vw, br	570 vw, br			
698[i] m	666[i] w, br	650 vw, br			
867 w, br					
1088[i] s					

[a] Experimental conditions as under Materials and Methods and in Figures 2 and 3. [b] In acetonitrile solution. [c] In an aqueous solution of 0.5 M HSpa, pH 8.6. [d] Measured for CpFd only—see Figure 2 and Materials and Methods. [e] This band is much stronger than the 145-cm^{-1} band of acetonitrile alone. Solvent bands are observed at 122, 392, 402, 780, and 923 cm^{-1}. [f] Abbreviations: s, strong; m, medium; w, weak; br, broad; sh, shoulder; v, very; e, extremely; n.d., not determined. [g] Raman band of ice. [h] ^{34}S* isotopic shift (cm^{-1}). [i] Bands involving mainly ligand modes, which are resonance enhanced compared to the corresponding bands of the ligand alone. Nonenhanced ligand bands are observed at 1000 and 1026 cm^{-1} for PhSH and 1270 cm^{-1} for HSpa.

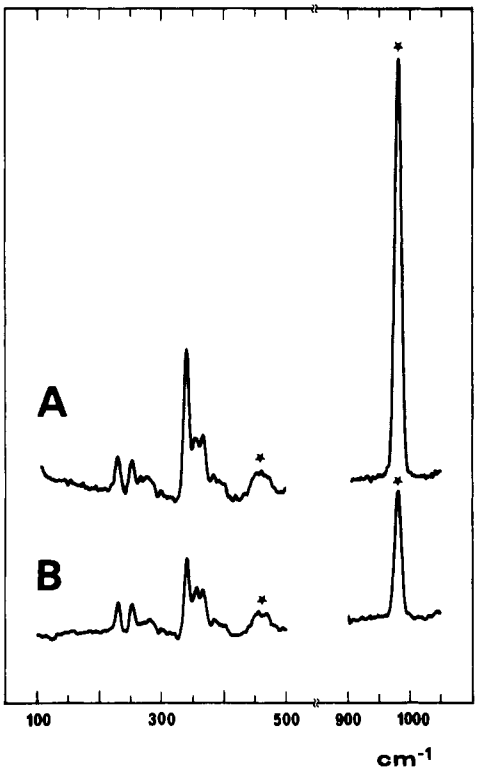

FIGURE 2: Depolarization ratio measurements on Raman bands of native Cp Fd. The excitation wavelength was 457.9 nm, the scanning speed 50 cm^{-1}/min, the time constant 1.8 s, the slit width 540 μm, and the temperature 30 K. The protein and ammonium sulfate concentrations were 6 mM and 2.6 M, respectively. (A) Scattered light analyzed parallel to the incident polarization. (B) Scattered light analyzed perpendicular to the incident polarization. The Raman bands of ammonium sulfate are starred.

conformational change of the [4Fe-4S] cluster at low temperature since the 30 and 300 K spectra are equally complex nor to any inequivalence of the two clusters in Cp Fd, since

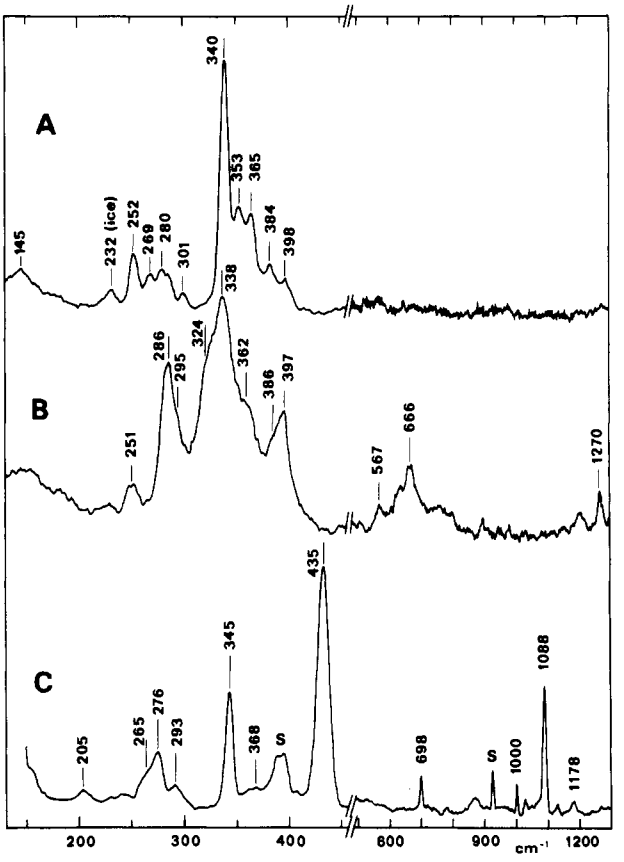

FIGURE 3: Resonance Raman spectra of native Cp Fd and Fe_4S_4 analogues. (A) Native Cp Fd 5 mM in 0.5 M phosphate buffer, pH 7.5, at 30 K. Four scans below 450 cm^{-1}; one scan above 500 cm^{-1}. (B) $[Fe_4S_4(Spa)_4][(C_2H_5)_4N]_2$, 15 mM, in a 0.5 M aqueous solution of HSpa, pH 8.6. T = 27 K; six scans. (C) $[Fe_4S_4(SPh)_4]$-$[(C_2H_5)_4N]_2$, 20 mM, in acetonitrile solution at 24 K; three scans. Conditions: excitation wavelength 457.9 nm, scanning speed 50 cm^{-1}/min, slit width 500 μm (600 μm for spectrum C), and time constant 1.8 s.

Table II: Resonance Raman Frequencies (cm^{-1}) of $[4Fe\text{-}4Se]^{2+}$ Clusters in Cp Fd and in Synthetic Analogues[a]

$Fe_4Se_4(SPh)_4^{2-}$ [b]	$Fe_4Se_4(Spa)_4^{2-}$ [c]	2[4Fe-4Se]$^{2+}$ Fd (^{76}Se)	isotopic shifts, $10^3 \times \Delta\nu/\nu$	depolarization ratios[d]	assignments, D_{2d}	
		146 vw				
	165 vw					
		174 (3[f]) w	17 ± 6	0.8 ± 0.15	E	Fe-Se*
184 ew[e]	186 vw	186 (3) w	16 ± 6	0.62 ± 0.22	B_2	Fe-Se*
205 w						
		216 (2) sh	9 ± 5	n.d.	E	Fe-Se*
218 m	218 s	224 (4) s	18 ± 5	0.34 ± 0.11	A_1	Fe-Se*
235 vw	236 m	240 (3) sh	13 ± 4	n.d.	B_1	Fe-Se*
260 w	289 vw	287 (5) m	17 ± 4	0.46 ± 0.11	A_1	Fe-Se*
		301 (4) vw	13 ± 3	n.d.	$B_2 + E$	Fe-Se*
		315 vw	n.d.	n.d.	$B_2 + E$	Fe-Se*
		344 (0) w sh	0	0.39 ± 0.2	E	Fe-Scys
	366[g]	360 (1) s	3 ± 3	0.28 ± 0.11	B_2	Fe-Scys
370 w		375 (0.5) s	1	0.28 ± 0.11	A_1	Fe-Scys
433 s						
480 vw, br	463 vw, br	455 vw, br				
530 w, br		530 vw, br				
		585 vw, br				
		648 vw, br				
698[h] w	665[h] w, br					
1088[h] s						

[a] Experimental conditions as under Materials and Methods and in Figures 4 and 5. [b] In acetonitrile solution. [c] In an aqueous solution of 0.5 M HSpa, pH 8.6. [d] Measured for CpFd only, on a ^{77}Se-substituted sample. [e] Abbreviations as in Table I. [f] $^{82}Se^*$ isotopic shifts (cm^{-1}). [g] Very broad (≃50 cm^{-1}) and complex feature. [h] Bands involving mainly ligand modes, which are resonance enhanced compared to the corresponding bands of the ligand alone. Nonenhanced ligand bands are observed at 1000 and 1026 cm^{-1} for PhSH. Solvent bands are present at 158, 392, 402, 780, 923, and 1043 cm^{-1}.

spectra containing the same number of bands have been obtained with *Bacillus stearothermophilus* Fd, which contains only one such cluster (Lutz et al., 1983).

Isotopic substitutions on the core sulfur atoms have been carried out in order to discriminate between modes predominantly involving Fe–S* or Fe–Scys bonds. In the 250–400-cm^{-1} region, the $^{32}S^* \rightarrow {}^{34}S^*$ substitution induces a shift of eight bands to lower frequencies (Table I). The relative shifts range from 1.3 to 2.0%, values that are close to those calculated for an isolated Fe–S harmonic oscillator by using Hooke's law (1.8%). On the other hand, the 353–365-cm^{-1} doublet remains almost unshifted. Such a clear-cut distinction between two groups of bands has also been observed in previous reports (Johnson et al., 1982b; Spiro et al., 1982).

Polarization measurements on the low-temperature RR spectrum of oxidized Cp Fd (Figure 2; Table I) show that five bands at 269, 340, 365, 384, and 398 cm^{-1} are polarized and that four bands at 252, 280, 286, and 353 cm^{-1} are depolarized or slightly anomalously polarized (252 cm^{-1}).

[4Fe-4S]$^{2+}$ Centers in Synthetic Analogues. (*a*) $[(C_2H_5)_4N]_2[Fe_4S_4(SCH_2CH_2CONH_2)_4]$. The title compound is very stable in slightly alkaline oxygen-free aqueous solutions containing an excess of the thiol ligand 3-mercaptopropionamide (Moulis & Meyer, 1982). The RR spectrum of $[Fe_4S_4(Spa)_4]^{2-}$ (Figure 3B) displays the same general structure as that of oxidized Cp Fd (Figure 3A). Therefore, the 457.9 nm excited RR spectra of the protein and of the synthetic analogue are likely to involve nearly the same electronic transitions of the $[4Fe\text{-}4S]^{2+}$ clusters. The latter conclusion may also be inferred from the great similarity of the electronic spectra of the protein and of the title compound at room temperature (Moulis & Meyer, 1982).

The differences occurring between RR spectra of the protein and of the water-soluble synthetic analogue consist of small frequency differences between homologous bands, probably not exceeding 4 cm^{-1} except for the 324-cm^{-1} band of $[Fe_4S_4(Spa)_4]^{2-}$, and differences in the relative intensities of some bands at ca. 285 and 390 cm^{-1} (parts A and B of Figure 3). Also, in the 350–400-cm^{-1} region, the bands of the synthetic analogue are less resolved than those of the protein, suggesting some line broadening in the former case. At higher frequencies (up to 1300 cm^{-1}), the spectrum of the synthetic analogue displays several broad weak to medium bands, in particular at 567, 666, and 1270 cm^{-1} (Figure 3B).

(*b*) $[(C_2H_5)_4N]_2[Fe_4S_4(SC_6H_5)_4]$. This cluster is one of the best characterized synthetic analogues of [4Fe-4S] ferredoxin centers, and among numerous other data, electronic spectra (DePamphilis et al., 1974; Cambray et al., 1977) and tridimensional structures (Que et al., 1974; Laskowski et al., 1978) are available for two of its redox levels. The low-temperature, 457.9 nm excited RR spectrum of $[Fe_4S_4(SPh)_4]^{2-}$ in acetonitrile solution (Figure 3C) significantly differs from those of Cp Fd and of the water-soluble synthetic analogue by its containing a smaller number of bands in the low-frequency region (Figure 3; Table I). Two strong bands are observed at 345 and 435 cm^{-1} and two weak to medium bands at 293 and 276 cm^{-1}, the latter with a shoulder at 265 cm^{-1}. Several other bands arise from the solvent, but the sharp one at 145 cm^{-1} is enhanced compared to that of acetonitrile alone. At higher frequencies, two bands at 698 and 1088 cm^{-1} (Figure 3C) are of particular interest, as they are not solvent lines and display markedly enhanced intensities compared to those of benzenethiol alone.

[4Fe-4Se]$^{2+}$ Centers of Cp Fd. In Cp Fd, the substitution of the bridging sulfur by selenium results not only in an overall frequency downshift but also in an extensive change of the RR pattern: whereas the spectrum of native Cp Fd is dominated by a single band at 340 cm^{-1}, the spectrum of Se-substituted Cp Fd is characterized by three groups of strong bands at ca. 370, 280, and 220 cm^{-1} (Figure 4A; Moulis et al., 1984). In spectra of monoisotopic ^{76}Se- or ^{82}Se-substituted Cp Fd samples (Figure 5), certain bands are better resolved than in spectra of natural abundance Se-substituted Cp Fd (Figure 4A), which contains significant proportions of five Se isotopes. Eleven bands are detected between 170 and 400 cm^{-1} (Table II). Several additional weak lines probably occur below 150 cm^{-1} (Figure 4A). They, however, are largely obscured by the rising background. At frequencies higher than ca. 400

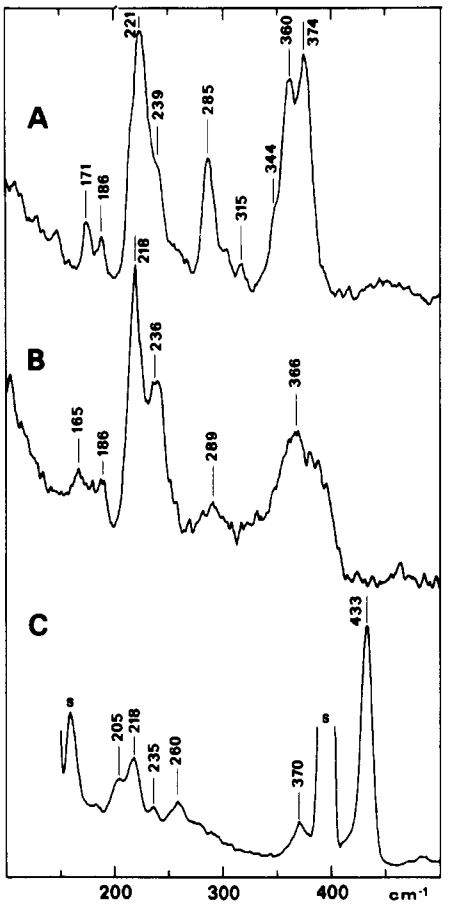

FIGURE 4: Resonance Raman spectra of Se-substituted Cp Fd and Fe_4Se_4 analogues. (A) Se-substituted Cp Fd (natural abundance Se), 15 mM, in 0.8 M phosphate buffer, pH 7.5, at 25 K; six scans. (B) $[Fe_4Se_4(Spa)_4][(C_2H_5)_4N]_2$, 10 mM, in a 0.5 M aqueous solution of HSpa, pH 8.6. T = 25 K; nine scans. (C) $[Fe_4Se_4(SPh)_4]$-$[(C_2H_5)_4N]_2$, 15 mM, in acetonitrile solution at 23 K; three scans. Other conditions as in Figure 3.

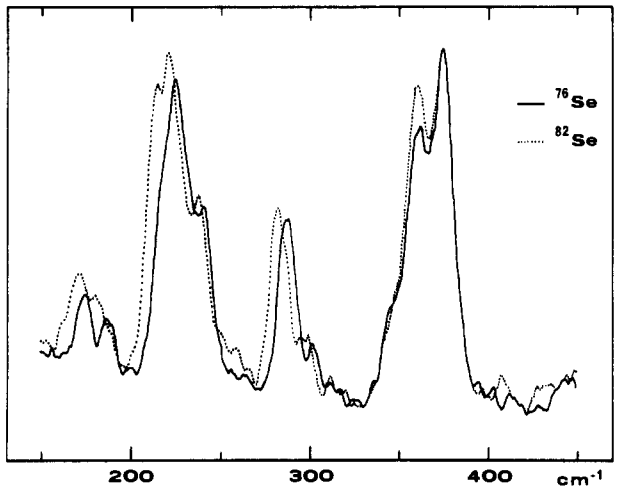

FIGURE 5: $^{76}Se^* \rightarrow {}^{82}Se^*$ isotopic shifts of the Raman bands of Se-substituted Cp Fd. (—) ^{76}Se (99.5%)-enriched Fd, 24 mM; nine scans. (···) ^{82}Se (92%)-enriched Fd, 17 mM; nine scans. The temperature was 20 K and other conditions were as in Figure 3A.

cm^{-1}, weak and broad features are present at ca. 450, 530, 585, and 650 cm^{-1}, as in the spectrum of native Cp Fd (Moulis et al., 1984).

Upon $^{76}Se^* \rightarrow {}^{82}Se^*$ isotopic substitution on the bridging selenium atoms, only the 344–375-cm^{-1} group of bands remains invariant (Figure 5; Table II). All other bands are shifted by amounts close to the value (1.6%) calculated for a diatomic Fe–Se molecule by using Hooke's law (Table II). Hence, as in the case of native Cp Fd, sensitivity to the mass of the core chalcogenide atoms allows a clear-cut discrimination between two groups of bands.

Polarization measurements were carried out on a ^{77}Se-enriched sample of 2[4Fe-4Se] Cp Fd (Table II). Four polarized bands are observed at 224, 287, 360, and 375 cm^{-1}, while two others at 185 and 174 cm^{-1} are depolarized and anomalously polarized, respectively. For most of the remaining bands, depolarization ratio measurements are more uncertain, due to their clustering in groups.

[4Fe-4Se]$^{2+}$ Centers in Synthetic Analogues. (*a*) $[(C_2H_5)_4N]_2[Fe_4Se_4(SCH_2CH_2CONH_2)_4]$. A RR spectrum of the title compound in a frozen aqueous solution containing excess free thiol is shown in Figure 4B. It closely resembles the spectrum of 2[4Fe-4Se] Cp Fd, with band frequencies matching within a very few wavenumbers (Table II). A few noteworthy differences are seen with respect to the relative band intensities: the ca. 285-cm^{-1} band, though present, is considerably weaker in the synthetic cluster. The group of bands centered at ca. 365 cm^{-1} is weaker and is about 2 times broader than in the protein spectrum. A weak and broad band is also observed at ca. 660 cm^{-1}, as in the case of the [4Fe-4S]$^{2+}$ water-soluble synthetic analogue.

(*b*) $[(C_2H_5)_4N]_2[Fe_4Se_4(SC_6H_5)_4]$. The RR spectrum of $[Fe_4Se_4(SPh)_4]^{2-}$ in frozen acetonitrile solution (Figure 4C) displays less bands in the 150–400-cm^{-1} region than the spectra of other [4Fe-4Se]$^{2+}$ clusters (Figures 4A,B). Weak to medium bands occur at 205, 218, 235, 260, and 370 cm^{-1}. A strong band is present at 433 cm^{-1}, close to the 435-cm^{-1} band of $[Fe_4S_4(SPh)_4]^{2-}$. At higher frequencies, the two bands at 698 and 1088 cm^{-1} do not arise from the solvent and display the same relative intensities as the homologous bands of $[Fe_4S_4(SPh)_4]^{2-}$ (Figure 3C).

Discussion

In the frequency ranges investigated in detail here, 250–400 cm^{-1} for the native Fd and 150–380 cm^{-1} for the Se-substituted Fd, all the bands sensitive to isotopic substitutions on core chalcogenide atoms are shifted by amounts very close to the values expected for a diatomic Fe–X harmonic oscillator (Tables I and II). These bands are located in the frequency range where Fe–X stretching modes have been observed in various compounds (Schmidt & Müller, 1974) and little doubt remains that they mainly involve stretching modes of the cubane $Fe_4X_4(S-)_4$ structure. Therefore, our subsequent analysis will be essentially concerned with these modes.

Previously published RR spectra of Cp Fd displayed only six bands in the Fe–S stretching region and were thus reasonably assigned in T_d symmetry, with two modes (A_1, T_2) principally involving stretching of the Fe–Scys bonds and four (A_1, E, $2T_2$) involving stretching of the inorganic Fe_4S_4 core (Spiro et al., 1982). Recently, however, the number of bands observed in the Fe–S stretching frequency range has been increased to 9 (Johnson et al., 1983) and 10 (Lutz et al., 1983; this work). A point group of symmetry lower than T_d has therefore to be used for the assignments (Table III). A number of crystal structures of [4Fe-4S] proteins (Stout, 1982) and of $[Fe_4X_4(SR)_4]^{2-}$ synthetic analogues (Berg & Holm, 1982) are now available. In all cases the idealized T_d structure undergoes a tetragonal distortion of the [4Fe-4X] core along four roughly parallel Fe–X bonds, which lowers the symmetry down to D_{2d}. Moreover, some spectroscopic data suggest that this distortion is conserved in frozen solution (Mascharak et al., 1983). In *Peptococcus aerogenes* Fd and in *Chromatium* HiPIP an additional trigonal distortion has been detected,

Table III: Stretching Modes Expected for $Fe_4X_4(S_t-)_4$ Clusters in T_d and in Lower Symmetry Point Groups

	T_d[a]	D_{2d}	S_4	D_2	C_{2v}	C_2	C_s
Fe–S_t stretching modes	A_1	A_1	A	A	A_1	A	A′
	T_2	B_2	B	B_1	A_1	A	A′
		E	E	B_2	B_1	B	A″
				B_3	B_2	B	A″
Fe–X stretching modes	A_1	A_1	A	A	A_1	A	A′
	E	A_1	A	A	A_1	A	A′
		B_1	B	A	A_2	A	A″
	T_1[b]	A_2[b]	A	B_1	A_2	A	A′
		E	E	B_2	B_1	B	A′
				B_3	B_2	B	A″
	$2T_2$	$2B_2$	2B	$2B_1$	$2A_1$	2A	2A′
		2E	2E	$2B_2$	$2B_1$	2B	2A′
				$2B_3$	$2B_2$	2B	2A″
modes active in the normal Raman effect	6	11	12	16	16	16	16
totally symmetric modes	2	3	4	4	6	8	10

[a] Maroni & Spiro (1968); Spiro et al. (1982). [b] Inactive in the normal Raman effect.

which involves an elongation of one of the principal S*··· Fe–Scys diagonals and leaves a mirror plane as the only symmetry element for the set of 12 atoms, thus decreasing the point group symmetry of the cluster to C_s (Carter, 1977b). As a trigonal distortion alone, i.e., in the absence of a tetragonal distortion, has not been detected in any crystallographic investigation of [4Fe-4X] clusters, it is probably not justified to consider C_{3v} as the relevant symmetry point group for assigning RR spectra of these clusters. Rather, the apparent ubiquity of the tetragonal distortion indicates that D_{2d} is the basic, highest symmetry point group to be considered in performing these assignments. Any additional distortion of the cluster should then lower the symmetry to one of the subgroups of D_{2d}. The Raman active stretching modes for $Fe_4X_4(S-)_4$ clusters in subgroups of D_{2d} are given in Table III. In D_{2d} symmetry, the eleven Raman active stretching modes include three ν(Fe–SR) modes and eight ν(Fe–X*) modes. Interestingly, these values match the numbers of bands that are unshifted and shifted, respectively, upon isotopic substitution on core chalcogenide atoms in both the native and the Se-substituted Fd (Tables I and II). Furthermore, the spectra of the proteins bear close similarity to those of the corresponding water-soluble synthetic clusters, which are expected to assume symmetries not substantially lower than D_{2d} (Mascharak et al., 1983).

Inspection of the scattering tensors of the Raman-active species of the D_{2d} point group (Mc Clain, 1971) shows that the modes belonging to these species can be distinguished according to the values of their depolarization ratios. These values measured at a given excitation wavelength (here 457.9 nm) should then, in general, permit discrimination between A_1 ($0 < \rho < {}^3/_4$), B_1–B_2 ($\rho = {}^3/_4$), and E (${}^3/_4 < \rho < \infty$) modes in the present spectra. It may be noted from Tables I and II, however, that the numbers of polarized RR bands of both the native and the Se-substituted Fd exceed those of the A_1 modes expected in D_{2d} symmetry (Table III), even if experimental uncertainties on the measurements are taken into account. This should not be taken as evidence that the ground-state symmetry of the [4Fe-4S] cluster of Cp Fd is actually lower than D_{2d}, since polarization dispersion of RR bands in apparent contradiction with the assessed symmetry point group of the molecule in its ground state has been observed, for instance, in porphin (Plus & Lutz, 1974) and in mesoporphyrin dimethyl ester (Plus & Lutz, 1975) excited in the region of band IV, as well as in cytochrome *c* (1360-cm^{-1} band) excited in the β band (Collins et al., 1973). Interference effects due to resonance with more than one electronic excited state may explain this phenomenon (Mortensen & Hassing, 1980), if, for example, in certain of these excited states, the molecule assumes symmetries lower than that of the ground state. In the present case of the [4Fe-4X] clusters of Cp Fd, polarization dispersion may well explain that the number of polarized RR bands observed is greater than expected for D_{2d} symmetry, since the 457.9-nm excitation is likely to involve several electronic excited states (Johnson et al., 1982a). Hence, in the following, RR spectra of Cp Fd will be assigned within the framework of a D_{2d} point group.

Assignments for the Fe–Scys Modes. Two RR bands of Cp Fd (Figure 3A), at 353 and 365 cm^{-1}, show no or very small isotopic shifts upon $^{32}S^* \rightarrow {}^{34}S^*$ substitution (Table I). They are therefore attributed to Fe–Scys stretching modes. This result confirms the former observation of a 357 cm^{-1} RR band in liquid solution spectra of Cp Fd, which was unaffected by bridging $^{34}S^*$ substitution (Johnson et al., 1982b).

In the D_{2d} point group, three ($A_1 + B_2 + E$) stretching modes of the Fe–Scys bonds are expected to be Raman active (Table III). The 353-cm^{-1} RR band of Cp Fd (Figure 3A) has a counterpart at 356 cm^{-1} in the IR (A_1 modes inactive) spectrum of $[Fe_4S_4(SCH_2Ph)_4][(C_2H_5)_4N]_2$ (Spiro et al., 1982) and has a depolarization ratio that is higher than that of the 365-cm^{-1} line and that may be close to 0.75. The 353-cm^{-1} band of Cp Fd is therefore assigned to a non totally symmetric mode (B_2 or E). The 365-cm^{-1} polarized band is attributed to the totally symmetric (A_1) terminal stretching mode. The second non totally symmmetric mode is thus missing in these spectra. This may result either from degeneracy of the B_2 and E modes or from an accidental coincidence between one of these two bands and the strong 340-cm^{-1} band.

In RR spectra of 2[4Fe-4Se] Cp Fd, two bands at 375 and 360 cm^{-1}, and a shoulder at 344 cm^{-1}, are largely insensitive to $^{76}Se^* \rightarrow {}^{82}Se^*$ isotopic substitution (Figure 5; Table II). They are therefore attributed to Fe–Scys stretching modes. The 375- and 360-cm^{-1} bands both are polarized, whereas only one totally symmetric mode (A_1) is expected in D_{2d} symmetry. As discussed above, this discrepancy may well arise from polarization dispersion.

At those frequencies corresponding to Fe–Scys stretching modes of the ferredoxins, medium to strong bands are observed in RR spectra of $[Fe_4X_4(Spa)_4]^{2-}$, but very weak lines only are detected at 368 cm^{-1} for $[Fe_4S_4(SPh)_4]^{2-}$ and at 370 cm^{-1} for $[Fe_4Se_4(SPh)_4]^{2-}$ (Figures 3 and 4; Tables I and II). We propose that the strong 435-cm^{-1} band, which is only slightly shifted (−2 cm^{-1}) upon replacement of the core sulfur atoms by selenium, which has no homologue, neither in spectra of alkylthiolate-liganded clusters (Tables I and II) nor in spectra of free benzenethiol (not shown), and which is much stronger than thiophenol bands (see below), arises from a mode predominantly involving Fe–S_t stretching. Indeed, in the case of the two aryl derivatives, the benzene π electrons may be partly delocalized toward the electrophilic $[Fe_4X_4]^{2+}$ core, which would result in a strengthening of the Fe–SR bonds and in upshifts of Fe–SR stretching modes of the $[Fe_4X_4(SPh)_4]^{2-}$ compounds. Evidence for electronic coupling between the $[Fe_4X_4]^{2+}$ core and the thiophenolate ligand is brought forth by the resonant enhancement of the 698- and 1088-cm^{-1} bands of the latter compared to their homologues in non resonant Raman spectra of the free thiol, taking its 1000- and 1026-cm^{-1} bands as internal standards (Figure 3C). The 698- and 1088-cm^{-1} bands of $[Fe_4X_4(SPh)_4]^{2-}$ can be attributed to A_1 (C_{2v}) modes of the thiophenolate ligand involving some C–S stretching character (Ham et al., 1960; Scott et al., 1956). The

Table IV: Relative Intensities of Totally Symmetric (A_1) Terminal and Bridging Modes as a Function of the Proximity of the Excitation Wavelength (4579 Å) to the Nearest Electronic Absorption Maximum

compound	λ_{max} (nm)	$\lambda_{exc} - \lambda_{max}$ (nm)	I(Fe–S_t)[a]/ I(Fe–X*)[b]	I(Fe–S_t)[a]/ I(Fe–X*)[c]
$Fe_4S_4(Spa)_4^{2-}$	375[d]	83	0.6	1
Cp Fd	388	70	0.4	3
$Fe_4S_4(SPh)_4^{2-}$	448[e]	10	2.2	5
$Fe_4Se_4(Spa)_4^{2-}$	373[d]	85	3.3	0.5
Se–Cp Fd	386	72	2	1
$Fe_4Se_4(SPh)_4^{2-}$	458[e]	0	10	4.2

[a] Peak height of the totally symmetric (A_1) Fe–S_t stretching mode at ca. 370 cm^{-1} for Fd and water-soluble synthetic analogues and at ca. 435 cm^{-1} for $[Fe_4X_4(SPh)_4]^{2-}$. [b] Peak height of the higher frequency totally symmetric (A_1) Fe–X* stretching mode (ca. 340 cm^{-1} for X = S and ca. 285 cm^{-1} for X = Se). [c] Peak height of the lower frequency totally symmetric (A_1) Fe–X* stretching mode (ca. 270 cm^{-1} for X = S and ca. 220 cm^{-1} for X = Se). [d] Moulis & Meyer (1982). [e] In acetonitrile solution.

alkylthiolate-liganded $[Fe_4S_4(Spa)_4]^{2-}$ compound displays several broad and overlapping bands in the 500–700-cm^{-1} region (Figure 3B). The spectral features in the latter range suggest that overtones of the fundamental Fe–S stretching modes are probably involved. However, the broad 666-cm^{-1} band has a counterpart at 665 cm^{-1} in the spectrum of $[Fe_4Se_4(Spa)_4]^{2-}$ (Table II), and therefore it probably arises in part from a C–S stretching mode.

Assignments for the Fe_4X_4 Cores. Eight bands display large isotopic shifts upon bridging $^{32}S \rightarrow {}^{34}S$ or $^{76}Se \rightarrow {}^{82}Se$ substitution in 2[4Fe-4S] and in 2[4Fe-4Se] Cp Fd, respectively (Tables I and II). In D_{2d} symmetry, eight Raman-active stretching modes, including two totally symmetric (A_1) ones, are expected for the Fe_4X_4 cores (Table III).

In the RR spectrum of native Cp Fd, the strong 340-cm^{-1} band has a depolarization ratio of 0.26 (Figure 2; Table I) and is therefore attributed to a totally symmetric (A_1) mode. This assignment is in agreement with that previously proposed in T_d symmetry for $[Fe_4S_4(SCH_2Ph)_4]^{2-}$ on the basis of combined IR and RR data (Spiro et al., 1982). For the assignment of the second totally symmetric mode that, together with a B_1 mode, arises from the splitting of an E (T_d) mode (Table III), the polarization measurements leave three possible bands at 269, 384, and 398 cm^{-1}. The following observations show that the best candidate is the 269-cm^{-1} band: whereas spectra of Cp Fd (Figure 3A) and $[Fe_4S_4(Spa)_4]^{2-}$ (Figure 3B) display ten and eight bands, respectively, in the 250–450-cm^{-1} region, only five components of significant intensity (260, 275, 293, 345, and 435 cm^{-1}) are observed for $[Fe_4S_4(SPh)_4]^{2-}$ (Figure 3C). Since the two synthetic analogues are most likely assuming the same point group symmetry (Mascharak et al., 1983), the smaller number of bands observed in the RR spectrum of $[Fe_4S_4(SPh)_4]^{2-}$ is presumably due to the occurrence of a different resonance enhancement mechanism. Indeed, the vicinity of the excitation frequency (457.9 nm) to the electronic absorption maximum of $[Fe_4S_4(SPh)_4]^{2-}$ (Bobrik et al., 1978; see also Table IV) should favor resonance via A-term scattering, resulting in a selective enhancement of the totally symmetric modes. Conversely, for Cp Fd and $[Fe_4S_4(Spa)_4]^{2-}$ the electronic absorption maxima are not as close to the excitation frequency as those of the aryl derivatives (Table IV), and they display Raman spectra arising from more than just an A-type resonance, thus involving both totally symmetric and non totally symmetric modes (Tables I and II). In the RR spectrum of $[Fe_4S_4(SPh)_4]^{2-}$ (Figure 3C) the strongest bands are the 435-cm^{-1} band, assigned to a Fe–SPh stretching mode (see above), the 345-cm^{-1} band, which is homologous to the 340-cm^{-1} (A_1) mode of the protein, and the 276-cm^{-1} band. The latter band, in view of the most probable predominance of A-term scattering for $[Fe_4S_4(SPh)_4]^{2-}$, is assigned to the second totally symmetric (A_1) Fe–S* stretching mode. Therefore, the 269-cm^{-1} band of Cp Fd, which is the only polarized band below 300 cm^{-1}, is assigned to a totally symmetric (A_1) Fe–S* stretching mode. In D_{2d} point group symmetry, all of the remaining bands have to be attributed to non totally symmetric modes. The 384- and 398-cm^{-1} bands, the low depolarization ratios of which presumably arise from polarization dispersion, are tentatively assigned to a B_2 + E pair descending from a T_2 (T_d) mode. The latter attribution is consistent with the previous observation in spectra of $[Fe_4S_4(SCH_2Ph)_4]^{2-}$ of an IR-active 382-cm^{-1} band that was shifted upon $^{32}S^* \rightarrow {}^{34}S^*$ isotopic substitution and was assigned to a T_2 (T_d) mode (Spiro et al., 1982). The relatively isolated depolarized band at 252 cm^{-1}, which may be anomalously polarized, is assigned to an E mode, which, together with a Raman-inactive A_2 mode, arises from the splitting of a Raman-inactive T_1 (T_d) mode (Table III). The high-frequency pattern of the Cp Fd RR spectrum in the 350–400-cm^{-1} region (Figure 3A) suggests that bands are arranged in pairs due to a moderate splitting of T_2 (T_d) or E (T_d) modes upon lowering of the symmetry to D_{2d}. Assuming that significantly larger splittings do not occur at lower frequency, we tentatively assign the 280-cm^{-1} band to the B_1 mode, which, together with the 269-cm^{-1} A_1 mode, descends from the E (T_d) mode (Table III). The remaining 286- and 301-cm^{-1} bands are then attributed to a B_2 + E pair.

In the RR spectrum of Se-substituted CpFd, only two bands among those shifted upon $^{76}Se^* \rightarrow {}^{82}Se^*$ substitution are polarized (Table II): these two bands, at 285 and 221 cm^{-1} for natural abundance Se-substituted Cp Fd (Figure 4A), are therefore attributed to the two expected totally symmetric (A_1) Fe–Se* stretching modes. Polarization data are not available for certain of the remaining bands, and therefore only tentative assignments are given below. The two weak bands at 301 and 315 cm^{-1} (Figure 4A), which are on the high-frequency side of the polarized 285-cm^{-1} band, are attributed to a B_2 + E pair. They may be the counterparts of the 384- and 398-cm^{-1} bands, which, in the spectrum of native Cp Fd, are located on the high-frequency side of the polarized 340-cm^{-1} band (Figure 3A). In the RR spectrum of Se-substituted Cp Fd (Figure 4A), the anomalously polarized 174-cm^{-1} band and the depolarized 187-cm^{-1} band are good candidates for a B_2 + E pair. By analogy with the low-frequency pattern in the 250-280-cm^{-1} region for native Cp Fd, the 215 and 239 cm^{-1} of Se-substituted Cp Fd, which occur on either side of the polarized 221-cm^{-1} band, are assigned to the remaining E and B_1 modes, respectively.

Although some assigments of non totally symmetric Fe–Se* modes could not be based on firm experimental grounds, it should be noted that the RR data on both ferredoxins are on the whole largely consistent with a ground-state D_{2d} symmetry. This is true in particular for the sets of depolarization ratios obtained at 457.9 nm, although some of these are most probably perturbed by properties of the resonant excited states of the chromophores.

Structural Implications. As interpreted in the preceding section, the present resonance Raman data provide information on the structure of [4Fe-4X] clusters in Cp Fd.

The Fe–Scys stretching modes of native and of Se-substituted Cp Fd have been identified by their insensitivity to isotopic substitutions on core chalcogenide atoms. These modes are observed at slightly higher frequency (by ca. 10 cm^{-1}) in

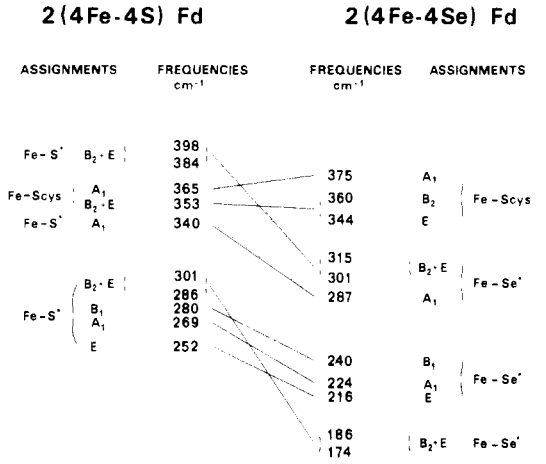

FIGURE 6: Assignments of stretching modes of the active site in D_{2d} symmetry for native and for ^{76}Se-substituted Cp Fd.

Se-substituted Cp Fd than in native Cp Fd. Presumably, a weaker coupling between the Fe–Scys and Fe–X modes occurs in the case of the former protein, due to the higher atomic weight of Se compared to S, which results in a larger reduced mass of the Fe_4Se_4 core. This should be reflected by a smaller sensitivity of the Fe–Scys stretching modes to isotopic substitution on Se* than on S* atoms. In both cases, however, the isotopic shifts are so small (≤ 1 cm^{-1}) that the differences observed between them (Tables I and II) are not significant.

The S* → Se* substitution results in large frequency downshifts of most modes corresponding to movements of the Fe_4X_4 core. In particular, the two totally symmetric Fe–X* stretching modes that have been independently assigned in both proteins, mainly on the basis of polarization measurements, are downshifted by 55 and 45 cm^{-1} (Figure 6) upon S* → Se* substitution. The assignments proposed for the non totally symmetric modes are indicative, for most of them, of downshifts similar to those of the totally symmetric modes (Figure 6). It thus appears that the S* → Se* substitution results in only a moderate reshuffling of the stretching modes of the Fe_4X_4* core, despite the large mass difference between the two chalcogenides. In addition to these frequency shifts, the S* → Se* substitution results in significant changes in relative intensities of various bands (Figures 3 and 4; Tables I and II). It has previously been shown that the Raman scattering cross sections of the Fe–Scys stretching modes are much the same in native and in Se-substituted Cp Fd (Moulis et al., 1984). The observed changes in relative intensities must therefore be ascribed to the Fe–X* stretching modes: this is probably due to shifts of X* → Fe charge transfer bands in the electronic spectra, although the general shape of the latter is not modified by the S* → Se* substitution (Bobrik et al., 1978; Meyer & Moulis, 1981).

The 4579 Å excited RR spectra of $[Fe_4X_4(SPh)_4]^{2-}$ compounds have been found to display band enhancement essentially via A-term scattering, and this property has been used, in combination with depolarization measurements, to assign the totally symmetric modes of the other clusters. Another peculiarity of the arylthiolate-liganded clusters is the occurrence of electronic coupling between the terminal Fe–SPh bonds and the thiophenol ligand. This coupling is reflected in the greater stability of such compounds in comparison with alkylthiolate liganded clusters (Que et al., 1974).

The spectra of $[Fe_4X_4(Spa)_4]^{2-}$ in aqueous solution display the same general pattern as those of the ferredoxins. However, some bands, in particular those assigned to Fe–Spa stretching modes, are significantly broadened, presumably due to intra- or intermolecular interactions assumed by the amide group of the 3-mercaptopropionamide ligand. These interactions may be analogous to those observed in $[(C_2H_5)_4N]_2[Fe_4S_4(SC-H_2CH_2OH)_4]$, where the hydroxyl groups of 2-mercaptoethanol participate in several intermolecular hydrogen bonds (Christou et al., 1981).

When considering $[Fe_4X_4(SPh)_4]^{2-}$, protein-bound [4Fe-4X] clusters, and $[Fe_4X_4(Spa)_4]^{2-}$ in aqueous solution, it appears that the larger the energy difference between the 370–470-nm electronic absorption maximum and the excitation frequency, the stronger the Raman bands assigned to modes of the Fe_4X_4 core, compared to those of terminal ν(Fe–S) modes (Table IV). This trend suggests that the electronic absorption bands of $[Fe_4X_4]^{2+}$ compounds peaking in the 370–470-nm region predominantly involve S_t → Fe charge transfer transitions near to their maxima and exhibit an increased X* → Fe charge transfer character at longer wavelength. This observation is in agreement with a previous report showing that the ca. 390-nm bands in UV–visible spectra of Cp Fd and of water-soluble synthetic analogues are unshifted upon S → Se substitution on core chalcogenides (Moulis & Meyer, 1982). Furthermore, in electronic spectra of $[Fe_4X_4(YPh)_4]^{2-}$ (X, Y = S, Se) compounds in DMF solution, the ca. 460-nm band is less shifted upon S → Se substitution on the core chalcogenide (458 → 466 nm) than on the ligand chalcogenide (458 → 478 nm) (Bobrik et al., 1978). Determination of excitation profiles and polarization dispersion of the RR active modes of the [4Fe-4X] clusters should yield detailed experimental data on the electronic structure of these entities.

The number of bands observed in RR spectra of Cp Fd, together with the crystal structures of various [4Fe-4X] clusters, have led us to choose D_{2d} as the local symmetry of the chromophores investigated here. Our experimental results are quite consistent with this choice and allow satisfactory band assignments. However, some of the present data may indicate distortions lowering the symmetry to a subgroup of D_{2d}. In particular, the number of polarized bands observed in 457.9 nm excited spectra is higher than expected in a strict D_{2d} frame (Tables I and II). Low depolarization ratios for non totally symmetric modes, resulting from polarization dispersion, can indeed also be interpreted in terms of additional ground-state distortions resulting, for example, for environmental interactions (Shelnutt, 1980; Zgierski & Pavlikovski, 1982). Nevertheless, these distortions are likely to be minor, since, otherwise, they would result in a greater number of RR-active stretching modes than actually observed (Table III). Therefore, it appears that the trigonal distortion evidenced in the crystal structures of [4Fe-4S] proteins (Carter, 1977b), which results in C_s local symmetry of the chromophore, is not a significant deformation in frozen solutions of Cp Fd. Indeed, in addition to other data, the marked similarities between the RR spectra of native and of Se-substituted Cp Fd on one hand and the RR spectra of the corresponding water-soluble synthetic analogues on the other hand (Figures 3 and 4) provide evidence that the protein-bound $[4Fe-4X]^{2+}$ clusters assume D_{2d} local symmetry.

The occurrence of the same D_{2d} symmetry for $[4Fe-4X]^{2+}$ clusters in proteins and in synthetic analogues suggests that this structural similarity may be extended to other redox levels. In particular, the elongation along the $\bar{4}$ (D_{2d}) axis that has been evidenced in synthetic analogues upon reduction to the $[Fe_4S_4]^+$ level (Laskowski et al., 1978) is likely to occur in Fd as well. However, additional interactions of the protein active sites with their environment during electron transfer cannot be ruled out, and the comparison of RR spectra of Fd in two

redox levels is expected to provide data relevant to this question.

Acknowledgments

We thank J. Roux for typing the manuscript and Dr. D. Tiede for kindly checking it.

Registry No. $[(C_2H_5)_4N]_2[Fe_4S_4(SCH_2CH_2CONH_2)_4]$, 93383-68-7; $[(C_2H_5)_4N]_2[Fe_4S_4(SC_6H_5)_4]$, 55663-41-7; $[(C_2H_5)_4N]_2[Fe_4Se_4(SCH_2CH_2CONH_2)_4]$, 93383-70-1; $[(C_2H_5)_4N]_2[Fe_4Se_4(SC_6H_5)_4]$, 93383-71-2; ^{34}S, 13965-97-4; ^{76}Se, 13981-32-3; ^{82}Se, 14687-58-2; ^{77}Se, 14681-72-2.

References

Adman, E. T., Sieker, L. C., & Jensen, L. H. (1976) *J. Biol. Chem. 251*, 3801–3806.

Berg, J. M., & Holm, R. H. (1982) in *Iron-Sulfur Proteins* (Spiro, T. G., Ed.) pp 1–66, Wiley-Interscience, New York.

Bobrik, M. A., Laskowski, E. J., Johnson, R. W., Gillum, W. O., Berg, J. M., Hodgson, K. O., & Holm, R. H. (1978) *Inorg. Chem. 17*, 1402–1409.

Cambray, J., Lane, R. W., Wedd, A. G., Johnson, R. W., & Holm, R. H. (1977) *Inorg. Chem. 16*, 2565–2571.

Carter, C. W., Jr. (1977a) in *Iron-Sulfur Proteins* (Lovenberg, W., Ed.) Vol. III, pp 157–206, Academic Press, New York.

Carter, C. W., Jr. (1977b) *J. Biol. Chem. 252*, 7802–7811.

Christou, G., & Garner, C. D. (1979) *J. Chem. Soc., Dalton Trans.*, 1093–1094.

Christou, G., Ridge, B., & Rydon, H. N. (1978) *J. Chem. Soc., Dalton Trans.*, 1423–1425.

Christou, G., Garner, C. D., Drew, M. G. B., & Cammack, R. (1981) *J. Chem. Soc., Dalton Trans.*, 1550–1555.

Collins, D. W., Fitchen, D. B., & Lewis, A. (1973) *J. Chem. Phys. 59*, 5714–5719.

DePamphilis, B. V., Averill, B. A., Herskovitz, T., Que, L., Jr., & Holm, R. H. (1974) *J. Am. Chem. Soc. 96*, 4159–4167.

Fee, J. A., Mayhew, S. G., & Palmer, G. (1971) *Biochim. Biophys. Acta 245*, 196–200.

Ham, N. S., Hambly, A. N., & Laby, R. H. (1960) *Aust. J. Chem. 13*, 443–455.

Johnson, M. K., Robinson, A. E., & Thomson, A. J. (1982a) in *Iron-Sulfur Proteins* (Spiro, T. G., Ed.) pp 367–406, Wiley-Interscience, New York.

Johnson, M. K., Spiro, T. G., & Mortenson, L. E. (1982b) *J. Biol. Chem. 257*, 2447–2452.

Johnson, M. K., Czernuszewicz, R. S., Spiro, T. G., Fee, J. A., & Sweeney, W. V. (1983) *J. Am. Chem. Soc. 105*, 6671–6678.

Laskowski, E. J., Frankel, R. B., Gillum, W. O., Papaefthymiou, G. C., Renaud, J., Ibers, J. A., & Holm, R. H. (1978) *J. Am. Chem. Soc. 100*, 5322–5337.

Lutz, M. (1977) *Biochim. Biophys. Acta 460*, 408–430.

Lutz, M., Moulis, J.-M., & Meyer, J. (1983) *FEBS Lett. 163*, 212–215.

Maroni, V. A., & Spiro, T. G. (1968) *Inorg. Chem. 7*, 188–192.

Mascharak, P. K., Hagen, K. S., Spence, J. T., & Holm, R. H. (1983) *Inorg. Chim. Acta 80*, 157–170.

Mc Clain, W. M. (1971) *J. Chem. Phys. 55*, 2789–2796.

Meyer, J., & Moulis, J.-M. (1981) *Biochem. Biophys. Res. Commun. 103*, 667–673.

Miller, G. A., Weiler, E. D., & Hausman, M. (1971) *J. Heterocycl. Chem. 8*, 581–586.

Mortensen, O. S., & Hassing, S. (1980) in *Advances in Infrared and Raman Spectroscopy* (Clark, R. J. H., & Hester, R. E., Eds.) Vol. IV, pp 1–60, Heyden and Son, Ltd., London.

Moulis, J.-M., & Meyer, J. (1982) *Biochemistry 21*, 4762–4771.

Moulis, J.-M., Meyer, J., & Lutz, M. (1984) *Biochem. J. 219*, 829–832.

Plus, R., & Lutz, M. (1974) *Spectrosc. Lett. 7*, 133–145.

Plus, R., & Lutz, M. (1975) *Spectrosc. Lett. 8*, 119–139.

Que, L., Jr, Bobrik, M. A., Ibers, J. A., & Holm, R. H. (1974) *J. Am. Chem. Soc. 96*, 4168–4178.

Schmidt, K. H., & Müller, A. (1974) *Coord. Chem. Rev. 14*, 115–179.

Scott, D. W., Mc Cullough, J. P., Hubbard, W. N., Messerly, J. F., Hossenlopp, I. A., Frow, F. R., & Waddington, G. (1956) *J. Am. Chem. Soc. 78*, 5463–5468.

Shelnutt, J. A. (1980) *J. Chem. Phys. 72*, 3948–3958.

Spiro, T. G., & Gaber, B. P. (1977) *Annu. Rev. Biochem. 46*, 553–572.

Spiro, T. G., Hare, J., Yachandra, V., Gewirth, A., Johnson, M. K., & Remsen, E. (1982) in *Iron-Sulfur Proteins* (Spiro, T. G., Ed.) pp 407–423, Wiley-Interscience, New York.

Stout, C. D. (1982) in *Iron-Sulfur Proteins* (Spiro, T. G., Ed.) pp 97–146, Wiley-Interscience, New York.

Sweeney, W. V., & Rabinowitz, J. C. (1980) *Annu. Rev. Biochem. 49*, 139–161.

Tang, S. P. W., Spiro, T. G., Antanaitis, C., Moss, T. H., Holm, R. H., Herskovitz, T., & Mortenson, L. E. (1975) *Biochem. Biophys. Res. Commun. 62*, 1–6.

Zgierski, M. Z., & Pavlikovski, K. M. (1982) *Chem. Phys. 65*, 335–367.